

Pacific Northwest National Laboratory

Operated by Battelle for the
U.S. Department of Energy

Direct Fast-Neutron Detection: A Progress Report

A.J. Peurrung
P. L. Reeder

R. R. Hansen
D. C. Stromswold

October 1998

Prepared for the U.S. Department of Energy
under Contract DE-AC06-76RLO 1830

DISCLAIMER

This report was prepared as an account of work sponsored by an agency of the United States Government. Neither the United States Government nor any agency thereof, nor Battelle Memorial Institute, nor any of their employees, makes any warranty, expressed or implied, or assumes any legal liability or responsibility for the accuracy, completeness, or usefulness of any information, apparatus, product, or process disclosed, or represents that its use would not infringe privately owned rights. Reference herein to any specific commercial product, process, or service by trade name, trademark, manufacturer, or otherwise does not necessarily constitute or imply its endorsement, recommendation, or favoring by the United States Government or any agency thereof, or Battelle Memorial Institute. The views and opinions of authors expressed herein do not necessarily state or reflect those of the United States Government or any agency thereof.

PACIFIC NORTHWEST NATIONAL LABORATORY
operated by
BATTELLE MEMORIAL INSTITUTE
for the
UNITED STATES DEPARTMENT OF ENERGY
under Contract DE-AC06-76RLO 1830

Printed in the United States of America

Available to DOE and DOE contractors from the
Office of Scientific and Technical Information, P.O. Box 62, Oak Ridge, TN 37831;
prices available from (615) 576-8401.

Available to the public from the National Technical Information Service,
U.S. Department of Commerce, 5285 Port Royal Rd., Springfield, VA 22161



This document was printed on recycled paper.

DISCLAIMER

Portions of this document may be illegible in electronic image products. Images are produced from the best available original document.

Direct Fast-Neutron Detection: A Progress Report

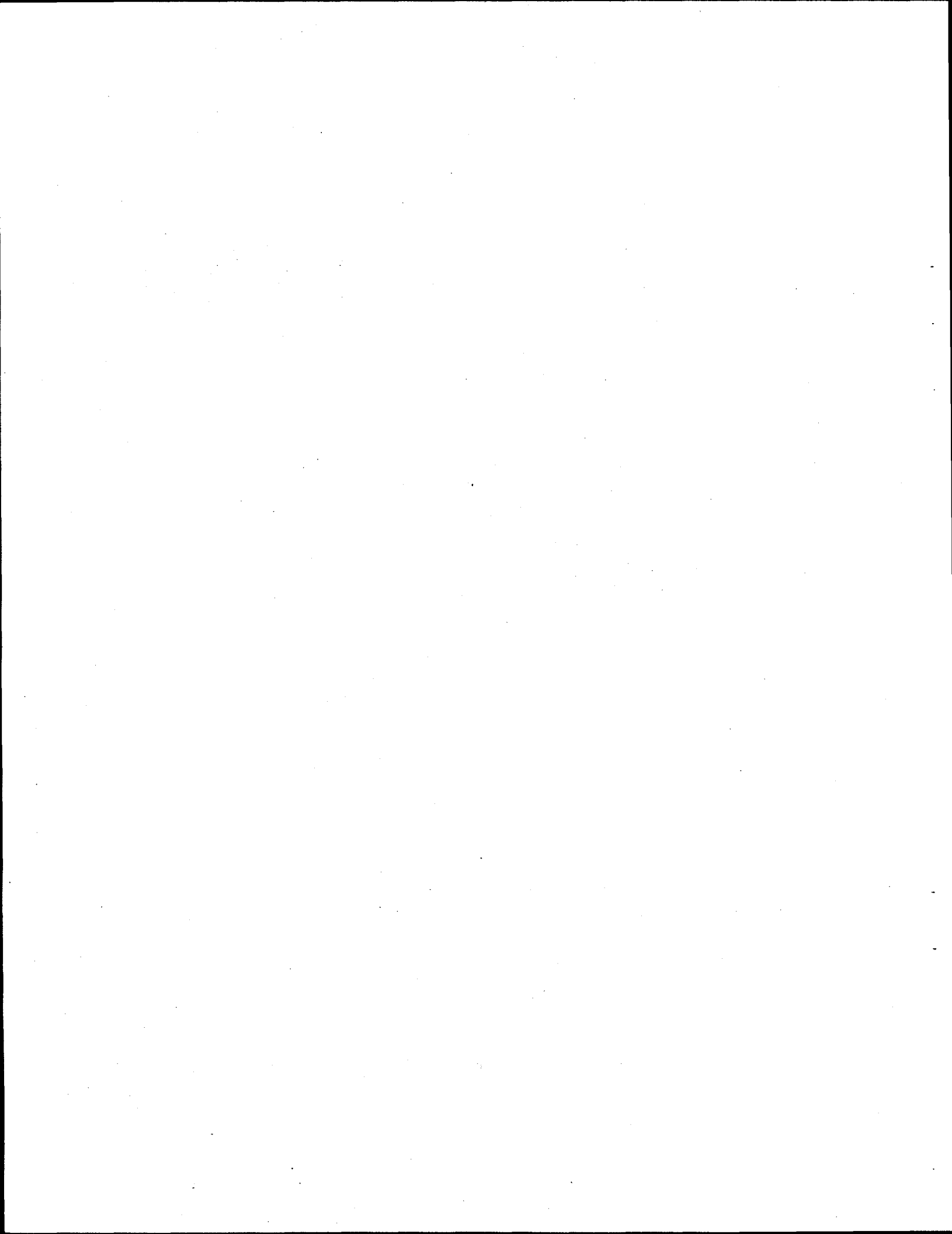
A.J. Peurrung
P. L. Reeder

R. R. Hansen
D. C. Stromswold

September 1998

Prepared for the U.S. Department of Energy
under Contract DE-AC06-76RLO 1830

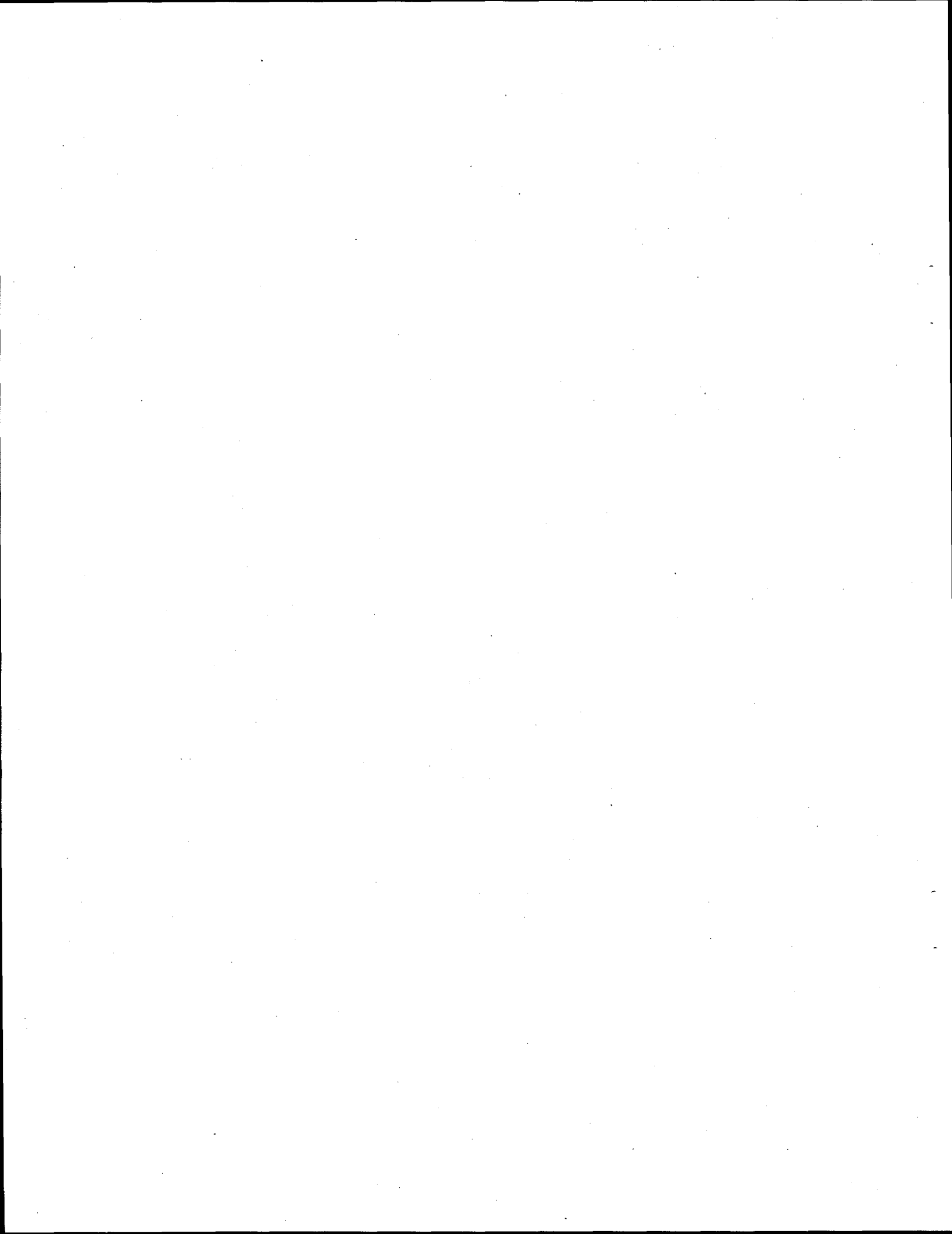
Pacific Northwest National Laboratory
Richland, Washington



Summary

It is widely acknowledged that future neutron-detection technologies will need to offer increased performance at lower cost. One clear route toward these goals is rapid and direct detection of fast neutrons prior to moderation. This report describes progress to date in an effort to achieve such neutron detection via proton recoil within plastic scintillator. Since recording proton-recoil events is of little practical use without a means to discriminate effectively against gamma-ray interactions, the present effort is concentrated on demonstrating a method that distinguishes between pulse types. The proposed method exploits the substantial difference in the speed of fission neutrons and gamma-ray photons. Should this effort ultimately prove successful, the resulting technology would make a valuable contribution toward meeting the neutron-detection needs of the next century.

This report describes the detailed investigations that have been part of Pacific Northwest National Laboratory's efforts to demonstrate direct fast-neutron detection in the laboratory. Our initial approach used a single, solid piece of scintillator along with the electronics needed for pulse-type differentiation. Work to date has led to the conclusion that faster scintillator and/or faster electronics will be necessary before satisfactory gamma-ray discrimination is achieved with this approach. Acquisition and testing of both faster scintillator and faster electronics are currently in progress. The "advanced" approach to direct fast-neutron detection uses a scintillating assembly with an overall density that is lower than that of ordinary plastic scintillator. The lower average density leads to longer interaction times for both neutrons and gamma rays, allowing easier discrimination. The modeling, optimization, and design of detection systems using this approach are described in detail.



Contents

1.0	Introduction	1.1
1.1	General Introduction to Direct Fast Neutron Detection	1.1
1.2	DFND via Proton Recoil in Scintillators	1.2
1.3	Applications	1.3
1.3.1	Coincidence Counting	1.4
1.3.2	Pulsed Active-Neutron Detectors	1.4
1.3.3	AmLi Active Neutron Detectors	1.4
1.3.4	Remote HEU Measurement	1.5
1.3.5	Fast-Neutron Imaging	1.5
2.0	The Initial Approach	2.1
3.0	Advanced Approaches	3.1
3.1	Multiple PMT Correlation	3.1
3.2	Fast PMT Tubes	3.1
3.3	Fast Scintillator	3.2
3.4	Low-Density Scintillating Assemblies	3.2
4.0	Conclusion	4.1
5.0	References	5.1

Figures

Figure 1.1. Diagram Showing the Repeated Interaction of a Neutron (left) and Gamma Ray (right) Along with the Pulse Shapes Expected for Each	1.3
Figure 1.2. Schematic Diagram Showing One Possible Implementation for a Fast Neutron Imager	1.6
Figure 2.1. Plot Showing 100 Experimentally Acquired Cerenkov Pulses and the Associated Width Spectrum	2.1
Figure 2.2. Plot Showing 100 Experimentally Acquired BC418 Scintillator Pulses Resulting from Gamma-Ray Radiation.....	2.2
Figure 2.3. Characterization of BC418 Scintillator via the “Single Photon” Method.....	2.4
Figure 2.4. Comparison of the Theoretically Expected Response of the PMT/Scintillator System with the Average Pulse Shape Actually Observed in Experiments	2.4
Figure 2.5. Histogram of the Pulse Widths for Sets of 100 Neutron and Gamma-Ray Pulses	2.5
Figure 2.6. Average Pulse Shape for the Widest 7 % of the Pulses Used for Figure 2.5	2.6
Figure 3.1. Neutron and Gamma-Ray Pulse Pairs for Bicron BC418 Plastic Scintillator.....	3.2
Figure 3.2. Geometry for Neutron-Proton Recoil Events, Along with a Polar Plot of the Scattering Probability as a Function of Scattering Angle	3.4
Figure 3.3. Gamma-Ray Time-of-Flight Spectrum Obtained for a ⁶⁰ Co Source with the Hardware and Electronics Anticipated for DFND Systems	3.5
Figure 3.4. Crude Demonstration of DFND Detection Obtained Using Two 10-cm × 10-cm × 1.5-cm Scintillating Slabs and a ²⁵² Cf Source	3.6
Figure 3.5. Percent of Neutrons that is Detected as a Function of the Dimensionless Ratio of the Square Slab Edge Length, l, to the Separation Distance, d, Between the Slabs	3.7
Figure 3.6. Calculated Detection Efficiency of a Two-Slab DFND System as a Function of the Thickness of the Front Slab	3.8
Figure 3.7. Calculated Relative Detection Efficiency of a Two-Slab DFND System as a Function of the Thickness of the Back Scintillator	3.9

1.0 Introduction

1.1 General Introduction to Direct Fast Neutron Detection

In its strict sense, the expression, "direct fast neutron detection (DFND)," refers only to a neutron-detection process that does not require moderation. The vast majority of neutron-detection applications use technologies where neutrons are moderated (slowed) and subsequently captured by a material such as ^3He , ^6Li , ^{10}B , Gd, or even ^{235}U . Each of these materials has a high cross section for neutron capture that leads to an energetic nuclear reaction. Note that any neutron-detection technology must not only record neutron interactions, but also provide a method for discriminating these interactions from the much more plentiful gamma-ray interactions that occur in any material. Generally speaking, conventional neutron-detection technologies work by arranging for the energy released in these nuclear reactions to be much higher than the energy imparted by gamma-ray interactions.

The motivation for DFND centers upon three basic factors of importance for applications: efficiency, cost, and information content. These factors are best explained by contrasting DFND with conventional neutron-detection technologies.

- **Efficiency** – The efficiency of DFND technology can, in principle, approach 100%. Suppose, for example, that a technology able to recognize proton recoil events as neutron events were operated within a 4-inch-thick slab of water. Roughly 95% of all normally incident 1-MeV neutrons will recoil at least once within such a slab (a bubble chamber may allow such a detection process, although at less than 100% duty cycle [Fisher et al. 1997]). In contrast, the efficiency of conventional neutron detection is determined largely by the efficiency of the moderation process and by the competition of materials such as hydrogen with the desired neutron-capture agent. Typically, moderation of neutrons leads to 50% loss. Of the remaining neutrons, typically the desired material only captures roughly 50%. Thus, typical efficiencies using the conventional approach are roughly 25%.
- **Cost** – DFND eliminates the need for isotopically pure materials such as ^3He , ^6Li , or ^{10}B . Thus, DFND may ultimately result in a significant reduction in the cost of neutron detection, especially when high-volume applications are considered. It should, however, be noted that the photomultiplier tubes (PMTs) necessary for our approach to DFND are likely to involve significant cost.
- **Information Content** – Conventional neutron detection provides no information beyond the approximate time at which a neutron event is recorded. Depending on the exact detector geometry, the timing information may be accurate to within 10 to 100 μs . No information is provided concerning the energy or incident direction of a particular recorded neutron. (Relatively crude, statistical statements can, of course, be made about a neutron population [Bramblett et al. 1960; Miller and Brugger 1985]). DFND, in contrast, has the potential to provide energy and direction information that would otherwise be lost during the moderation process. In addition, the much higher speed of fast neutrons results in a timing accuracy that is roughly 1 to 10 ns, or roughly 4 orders of magnitude faster than that provided by conventional approaches to neutron detection.

There are a limited number of possible differences between gamma-ray and neutron interactions that can be exploited to provide discrimination between the two types of events. Each of the approaches to DFND that has ever been attempted has made use of one of the following:

- **Track Length of Scattered Particle** – A 1.0-MeV recoil proton deposits energy much more rapidly than the corresponding 1.0-MeV photoelectron. The range of the proton in silicon is roughly 20 μm , whereas the range of the electron is roughly 2 mm, or 100 times further.

- **Availability of the Neutron for Capture** – There are nuclear reactions that a photon simply cannot induce, such as neutron capture.
- **Speed** – The speed of the photon is, of course, fixed at 30 cm/ns. The speed of a 1.0-MeV neutron is roughly 1.38 cm/ns, or roughly 22 times slower.

The list below describes several of the previous approaches that have been actively pursued for achieving DFND. While a number of these technologies have at some time found use for specific applications, none of them have the attributes necessary to realize all of the advantages listed above for DFND. A good, general discussion of fast neutron detection, much of which requires moderation, is found in chapter 15 of the textbook by G. F. Knoll (Knoll 1989).

- **Liquid Scintillators** – Some liquid scintillators have the special property that the pulse shape depends somewhat upon the charge-to-mass ratio of the particle-depositing energy ratio (Hentley et al. 1988; Moszynski et al. 1992; Kunze et al. 1995). Unfortunately, this method does not provide sufficient pulse-type discrimination at fission energies (0.5 to 2.0 MeV). Additionally, the need to integrate for 200 to 300 ns after an event leads to pulse corruption under high-rate conditions.
- **Foils** – DFND can be achieved using materials for which a particular activation reaction is either energetically forbidden or extremely unlikely without a flux of fission neutrons (Shleien 1992). While this method offers tremendous simplicity, no timing and little energy information is provided, and efficiencies are typically below 1%.
- **⁴He Detectors** – DFND systems have been constructed using proportional counters filled with ⁴He gas. This approach exploits the fact that only the neutron-induced recoil ⁴He nucleus (alpha particle) can deposit sufficient energy to exceed a properly selected threshold value (Atwater 1972). The efficiency offered by this method is severely limited by the relatively small amount of ⁴He gas that can be placed within a proportional counter.
- **Bubble Chambers** – The different energy deposition rates of the recoil proton and photoelectron make possible the development of bubble chambers in which a superheated liquid is induced to boil only as a result of neutron events (Ing et al. 1997; Fisher et al. 1997). While very little timing information is provided by this approach, energy and directional information are preserved. Discrimination against gamma-rays is effectively total. Bubble chambers are best analyzed after division into two distinct categories. Modern dosimetric bubble chambers (also called superheated droplet detectors) work by suspending superheated droplets within a matrix material. These detectors are simple and rugged, but have poor efficiency. A second type of bubble chamber uses a bulk fluid that spends only part of the time in a superheated state. These bubble chambers were used for particle-physics experiments before the advent of modern, solid-state particle detectors. While these bubble chambers are more complex, they offer the potential for nearly 100% efficiency.

1.2 DFND via Proton Recoil in Scintillators

The DFND approach discussed for the remainder of this paper involves recognition of repeated proton recoil in ordinary plastic scintillator. Proton recoil has long been an accepted method for neutron detection in situations where the identity of the interacting particle is already known (Curie and Joliot 1932). The high hydrogen content of plastic scintillator offers the potential of high efficiency. The relatively rapid response (~2 ns) of typical plastic scintillators offers the potential for highly accurate timing of neutron interactions. The cost of ordinary plastic scintillator is quite low, forming an insignificant contribution to the overall system cost when PMTs and electronics are taken into account.

For these reasons, it is expected that DFND via proton recoil may uniquely hold the advantages needed by a variety of neutron-detection applications.

The proposed technique for pulse-type discrimination exploits the difference in the speeds of the neutron and the photon as they travel between repeated interactions. A normally incident 1.0-MeV neutron has a greater than 90% chance of recoiling within a 10-cm-thick slab of plastic scintillator. Subsequent interactions occur with even greater probability, but are separated in time by roughly 3 ns. Because the neutron loses half of its energy on average in each collision, only the first two to three recoil events are likely to be of use. While gamma rays are also capable of repeated interaction, their high speed should result in the completion of any complex interaction in less than 1.0 ns. Figure 1.1 illustrates the proposed method for pulse discrimination. The use of low-density assemblies of plastic scintillator lengthens both the neutron and gamma-ray interaction timescales, but preserves the relative difference between the two. In its simplest form, the technique proposed here for pulse discrimination amounts to merely a complicated form of time-of-flight discrimination. Time-of-flight discrimination has been a mainstay of nuclear physics research for identifying particles whenever the timing of the initiating event is known (for example, Codino 1998). For DFND via proton recoil, the "initiating event" becomes the first of the repeated series of Compton-scatter events (photon) or proton-recoil events (neutron).

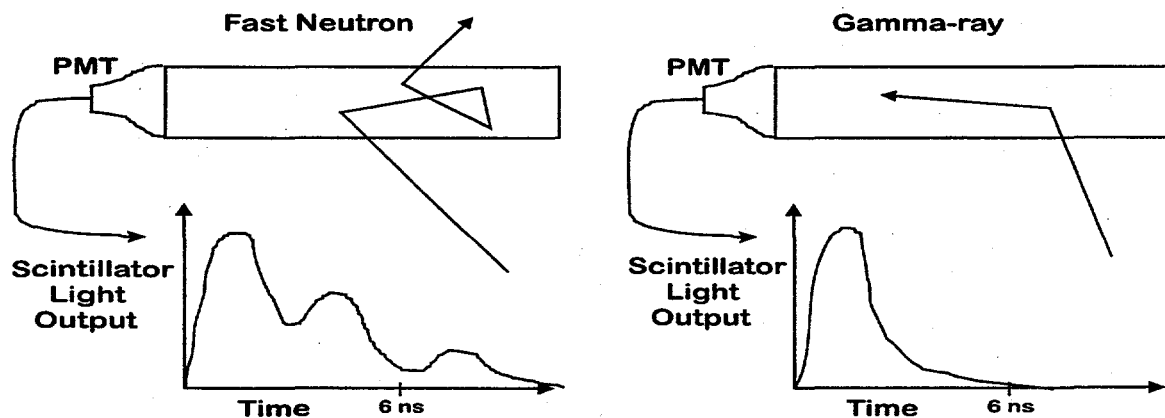


Figure 1.1. Diagram Showing the Repeated Interaction of a Neutron (left) and Gamma Ray (right) Along with the Pulse Shapes Expected for Each. This diagram assumes the existence of electronics sufficient to allow effective pulse discrimination.

Development of proton-recoil-based DFND requires a substantial intuition for the physics of proton-recoil events in plastic scintillator. A previous report (Peurrung et al. 1997) describes a number of theoretical and computational results concerning proton recoil in plastic scintillator. We continue to use MCNP neutron-transport code (Briesmeister 1993) to calculate the approximate pulse shapes expected for assemblies of plastic scintillator and the overall efficiency expected for particular configurations. Recent work has extended these calculations to the case of low-density scintillator assemblies. These results will be discussed in conjunction with the design of such DFND systems in Section III.

1.3 Applications

Should DFND technology development be successful, it may eventually displace conventional neutron-detection technologies for a number of applications simply on the basis of improved performance-to-cost ratio. In this section, we focus on five specific applications where DFND technology

has the potential either to significantly improve upon the capability of conventional neutron detection or to provide a capability that simply does not exist with current systems.

1.3.1 Coincidence Counting

The accidental count rate for any coincident detector is equal to $2R^2\tau$, where τ is the length of time used for the coincidence time window and R is the detection rate for "single" events. Because the time window for proton-recoil-based DFND may be as much as 4 orders of magnitude shorter than that of conventional neutron detection, accidental backgrounds may be dramatically lower. This improvement would allow more sensitive and/or more accurate detection of special nuclear materials. The improved timing may be especially critical for detectors that require coincidence between a neutron and a gamma ray.

1.3.2 Pulsed Active-Neutron Detectors

The differential die-away and shuffler techniques are active methods for measuring materials such as uranium for which the naturally emitted radiation is absent or hard to use. As normally implemented, these techniques use strong, pulsed neutron sources and a substantial moderating "cave" that surrounds the region containing materials or containers to be measured (Rinard et al. 1994 and references therein). Without fissile material present, the neutron flux decreases exponentially as the initially fast neutrons are moderated and captured. Any fissile material changes the time constant via the process of induced fission.

The challenge in differential die-away or shuffler measurements, as in any active technique, is rejection of those neutrons that are part of the interrogating source. Induced-fission neutrons provide all of the information desired for the measurement; interrogating neutrons provide no useful information. A successful DFND technology would strongly impact active measurement technology by offering two effective methods that discriminate between induced fission and interrogation neutrons:

- The accurate timing provided by DFND technology should make possible the coincident detection of induced fission neutrons. This is effectively impossible with conventional neutron-detection technologies.
- The energy information provided by DFND allows quite effective discrimination. Assuming that the interrogating neutrons initially have an energy of 14 MeV, six to eight proton recoils should be all that is required before the energy of the interrogating neutron population drops significantly below that of any induced fission neutrons that are produced. For a container that is roughly 1 meter in size, this energy reduction should be complete in less than 0.5 μ s. Thus, any *fast* neutrons detected after 0.5 μ s *must* be the result of induced fission.

1.3.3 AmLi Active Neutron Detectors

It would be very desirable for a variety of applications to be able to construct a portable (small, simple, lightweight) active detection system for confirmation of uranium material or components. Current active neutron-assay systems, such as differential die-away or shuffler systems, are large, complex, and expensive systems that are not suited for field use. Although instruments have been developed that do not require pulsed neutron sources (for example, Menlove 1979; Menlove 1981), these instruments continue to be relatively large and continue to require specific, favorable materials and geometry. DFND technology would allow the construction of portable and adaptable active systems, primarily because the energy information it provides allows effective rejection of interrogating neutrons. A simple AmLi neutron source has an average energy of 0.3 MeV and little or no neutron emission above 1.3 MeV. An energy threshold of roughly 1.5 MeV, therefore, should effectively reject interrogating neutrons while recording a significant fraction of induced fission neutrons.

1.3.4 Remote HEU Measurement

The differential die-away method discussed above may be sufficiently effective to allow measurement of HEU from distances as great as 25 meters or more. The principle remains the same. After roughly 10 us, a 14 MeV neutron has either traveled a distance of 500 meters, or has moderated to a significant extent. In either case, such a neutron will *not* be recorded by a DFND technology. Therefore, any recorded neutrons must be the result of induced fission. One of the primary limitations on this technology is the fact that the earth's crust contains a significant amount of natural uranium. In other words, detection of highly enriched uranium (HEU) at distances larger than about 50 meters is likely to fail with this technique simply because of "background" induced fission taking place in the earth's crust. (The top meter of soil within 100 meters of a given point contains on average 1.5 kg of ^{235}U !)

1.3.5 Fast-Neutron Imaging

While a number of attempts have been made in the past to achieve imaging neutron detection, none have the utility that this system should offer. Previous fast-neutron imaging detectors such as the "recoil telescope" (Knoll 1989) are notoriously inefficient and thus incapable of rapid data acquisition. A coded-array neutron imager developed at Brookhaven National Laboratory only records thermal neutrons and must therefore cope with the myriad problems associated with environmental moderation and air attenuation (Vanier et al. 1995). Because thermal neutrons are easily scattered, such a detector cannot image "through" other materials as would be allowed by a fast-neutron imager. While directional fast neutron detectors can and have been constructed using geometry or shielding, these systems do not acquire an image and tend to suffer from high backgrounds and imperfect directionality.

An example of a system that might use DFND technology to achieve efficient, fast neutron imaging is shown in Figure 1.2. This approach is fundamentally a straightforward combination of coded-array technology with DFND neutron detection. Coded-array imaging is a general technique in which the incident radiation is made to pass through a specially patterned, absorbing "mask," which casts a shadow onto a radiation detector that is capable of recording the two-dimensional location information. The pattern coded into the mask is specially chosen so that the shadow of a point source striking the radiation detector can be recognized using sophisticated mathematical analysis. This process not only allows the angular position of any radiation sources to be accurately calculated, but also provides a powerful method for reducing the effective radiation background. Simply put, the background can be effectively rejected because it does not share the spatial pattern that the mask imposes upon the "signal" neutron flux.

This DFND detection system shown in Figure 1.2 consists of two planar scintillators, where the first and smaller of the two planes is instrumented to allow localization of recoil events. The purpose of the second, larger plane is simply to provide pulse-type discrimination via the time-of-flight from the first recoil (or Compton scattering) event. Section III discusses the detailed properties of systems constructed using this approach to DFND.

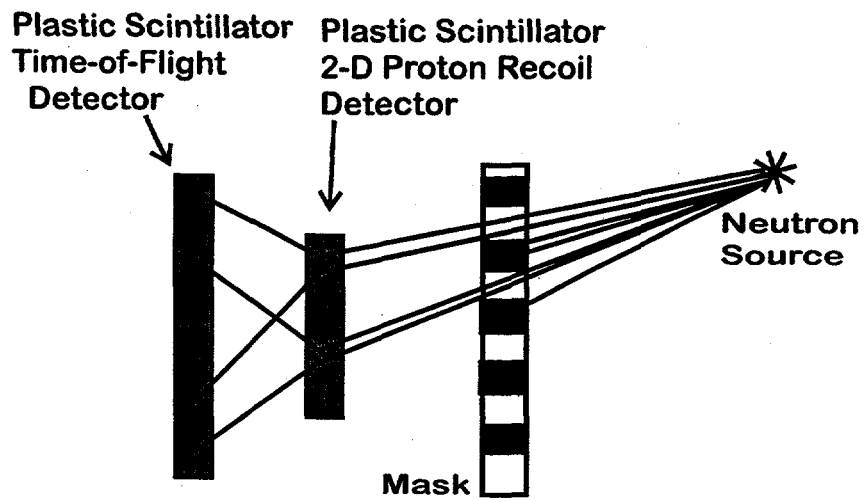


Figure 1.2. Schematic Diagram Showing One Possible Implementation for a Fast Neutron Imager. The three planes, moving right-to-left, are the coded mask, the start-trigger scintillator able to record proton recoil events with 2-D position resolution, and the stop-trigger scintillator able to record recoil events and reject gamma rays based on time-of-flight.

2.0 The Initial Approach

This section describes a series of investigations designed to assess and understand the performance of DFND systems consisting of a single, solid piece of ordinary plastic scintillator. In its simplest form, the detection system consists only of a piece of fast plastic scintillator and a fast PMT. A Tektronics TDS 684B digital oscilloscope (5×10^9 samples/s, 1 GHz) records the pulses arising from this system. A variety of radiation sources was used to produce pulses. When gamma-ray pulses were desired, a ^{137}Cs or ^{60}Co source was used. Strontium-90 sources were commonly used to provide beta radiation. Neutron pulses were acquired by using a time-of-flight identification system in conjunction with a ^{252}Cf source. (This is necessary because a "pure" neutron source does not exist – neutron capture always leads to some admixture of gamma rays near a neutron source.)

The most commonly used PMT for these studies was the 51-mm diameter Hamamatsu R2083 PMT, which is claimed to have a 0.7-ns rise time and a 0.37-ns transit time spread (typical). While this tube has a relatively high dark current, it is among the very fastest tubes available and was therefore well suited to these investigations. To test the performance of the PMT under conditions relevant to DFND, its impulse response was measured using Cerenkov radiation. Note that light generated in plastic or glass via Cerenkov radiation is generated "instantly" for all practical purposes. Thus, only optical travel delays and the response of the PMT determine the shape of Cerenkov pulses. Further, using a thin plastic slab in conjunction with a ^{90}Sr beta source ensures that optical delays are less than 0.1 ns. A set of 100 Cerenkov pulses is shown in Figure 2.1 along with a histogram of the full-width-half-maximum (FWHM) for this set of pulses. It is clear that the Cerenkov pulses are narrow and repeatable, with an FWHM close to 1.5 ns. These results are entirely consistent with the technical specifications of the PMT.

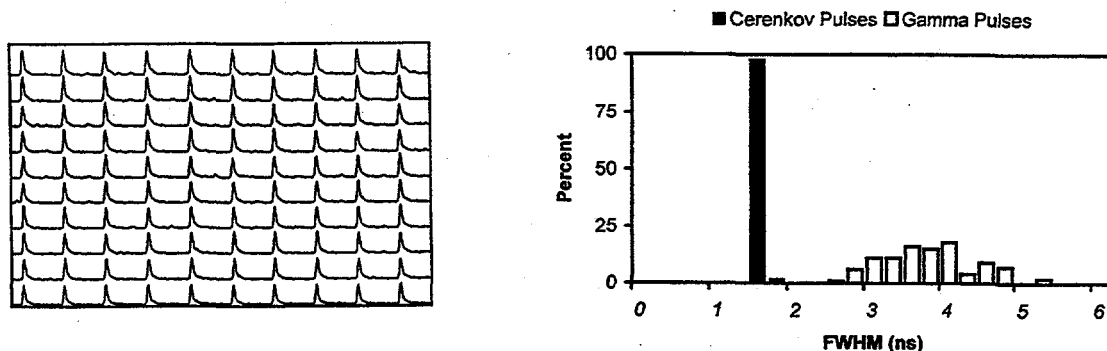


Figure 2.1. Plot Showing 100 Experimentally Acquired Cerenkov Pulses and the Associated Width Spectrum. The average width for this set is roughly 1.5 ns. The width spectrum for a typical set of gamma ray pulses is also shown for comparison.

An extensive series of investigations was carried out to characterize and understand the response of the scintillator to excitation. A typical result is shown in Figure 2.2. Note that the pulses shown in Figure 2.2 are not the sole result of the scintillator response. These pulses also involve the response of the PMT in addition to any optical broadening effects. Because the size of scintillators used was generally 7.5 cm or less, optical delays have only a slight effect on the pulse shape. (The speed of light within the scintillator is roughly 20 cm/ns.) However, we believe the varied shapes of the pulses shown in Figure 2.2 result primarily from the scintillator's response, both because the PMT response is known to be uniform and because of the extensive series of tests summarized below:

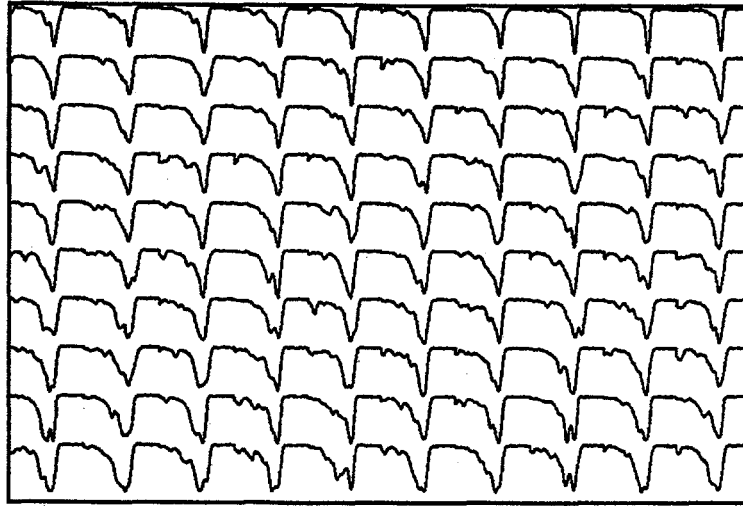


Figure 2.2. Plot Showing 100 Experimentally Acquired BC418 Scintillator Pulses Resulting from Gamma-Ray Radiation. The combined width and irregularity of these pulses hinder the effective recognition of neutron pulses.

- **Scintillator Size** – Tests were performed with scintillators of varying sizes ranging from less than 1 cm in thickness to the full 7.5 cm in thickness. The results showed that scintillator size had only a slight effect and that, as expected, thinner scintillators yielded slightly narrower pulses. This result supports a conclusion that optical effects are of minimal importance.
- **Scintillator Surface** – Tests were performed in which the optical characteristics of the scintillator surface were changed from predominantly reflective to predominantly absorbing. The pulse shapes for the two populations were again similar and again support the conclusion that optical effects are of only slight importance.
- **Scintillator Type** – Tests were performed using a number of different scintillator types. Most of the scintillators tested were from the standard line of Bicron scintillators, although at least one scintillator from Amcryst-H Corporation in the Ukraine was characterized. These results contained no surprises, showing that pulse widths depended upon the claimed scintillator response time in a logical fashion. One quenched scintillator, BC-422Q, was tested. This scintillator has a significantly faster response time (0.7 ns, compared to 1.5 ns and greater) than most scintillators, but has a correspondingly lower light output (roughly 20% as much). These pulses were considerably narrower, but their lower light output increases statistical fluctuations and thus hinders gamma-ray discrimination. The primary result of these tests was that all scintillator types share the general properties illustrated in Figure 2.2.
- **Liquid Scintillator** – Tests were performed on one sample of liquid scintillator to determine whether any significant difference existed between the response of liquid and solid (plastic) scintillators. As expected, the liquid-generated pulses were somewhat slower, but otherwise exhibited no significant differences.
- **Radiation Type** – This test compared the response of the scintillator to beta and gamma radiation. Because energy is deposited in the scintillator via fast electrons in both cases, differences in the

two populations must arise from the differing interaction physics. Only the gamma ray can scatter and thus interact at two different locations within the scintillator. The results indicated that differences between the pulse shapes for the two types of radiation were insignificant. We conclude from these results that the complex physics of gamma-ray interaction is not significantly responsible for the properties of the pulses observed in Figure 2.2.

- Interaction Energy – The general properties of pulses were studied as a function of the pulse energy (integrated area) for both gamma-ray and beta excitations. The results of these tests were in general complex and somewhat confusing. Although explanations are not available for all of the observed phenomena, several conclusions along with possible or partial explanations are given below:
 1. Deviations from the “average” pulse shape are greater for pulses of smaller energy. We believe this to be simply a result of the more varied statistics of pulses consisting of a relatively small number of photoelectrons.
 2. The average pulse FWHM exhibits a complex dependence on pulse energy and even on the particular gamma-ray source used. We believe this to be evidence that the FWHM is a poor measure for pulses that may consist of multiple “peaks.”
 3. For populations of relatively low-amplitude pulses, there is often a subset of pulses that are relatively narrow and consistent. These pulses may be the result of chance, or may result from complex behavior of the PMT when excited by light that is not “instantaneous.”

The complex results of the scintillator characterization tests described above served as motivation for a more precise characterization of the properties of the plastic scintillator used for DFND. Single photon tests were performed to allow measurement of the scintillator response in isolation (Moszynski 1982). In these tests, two different PMTs simultaneously view a scintillator. The first PMT records the entire pulse for the purposes of deriving an accurate timing signal representing the start of the excitation. The second PMT views the scintillator through a pinhole small enough to ensure that only a single photon will be recorded in the vast majority of cases. A histogram of the time difference between the start of the excitation and the arrival of photons accurately describes the scintillator response. Any effects arising within the PMT should be eliminated via this approach. The first PMT is only used to generate a timing signal, and the second PMT only records a single photoelectron. The results of a single photon characterization of Bicron BC418 scintillator are shown in Figure 2.3. These data are consistent with the previously published results (Lynch 1975; Moszynski and Bengtson 1977; Moszynski and Bengtson 1979) and with previous literature data describing Bicron scintillator. We conclude that the scintillator response is behaving as expected and cannot be faulted for the relatively broad and variable pulses shown in Figure 2.2.

Figure 2.4 compares the theoretically expected response of the PMT/scintillator system with the average pulse actually observed in experiments. The expected response is obtained as the mathematical convolution of the average Cherenkov pulse with the scintillator response as indicated by the single photon results. This convolved response is compared with the average scintillator response for large pulse energies. The agreement between the expected and observed pulse shapes is sufficiently good to conclude that our understanding of the pulse-generation process is adequate. However, the level of statistical variation, especially for the smaller pulses, is greater than was originally anticipated. This variation must arise from the random nature of photon emission, photon transport, photoelectron emission, and PMT pulse-generation processes. It is this pulse-to-pulse variation that most hinders our ability to identify neutron pulses by effectively distinguishing them from gamma-ray pulses. As indicated by Figure 2.2, a small but possibly significant number of the gamma-ray pulses may have a shape that mimics that of multiple proton-recoil neutron interactions.

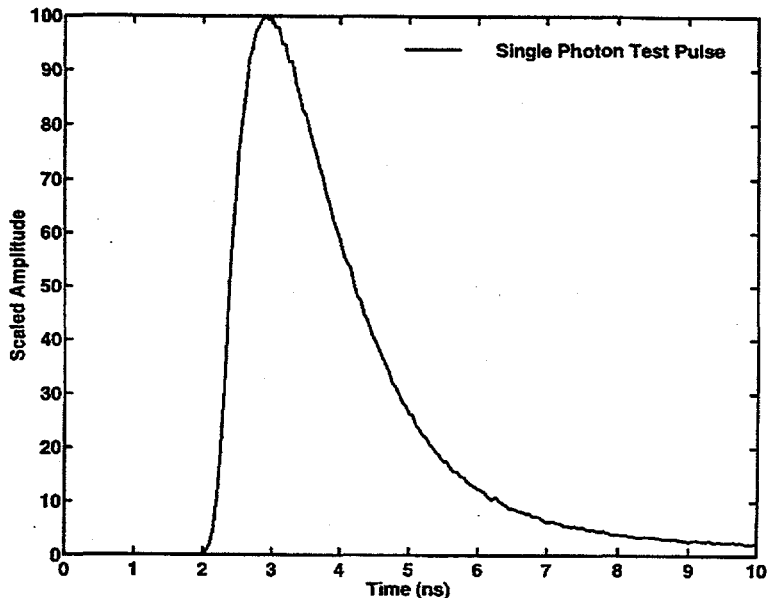


Figure 2.3. Characterization of BC418 Scintillator via the “Single Photon” Method. These results show adequate agreement with scintillator time profile previously obtained by other researchers.

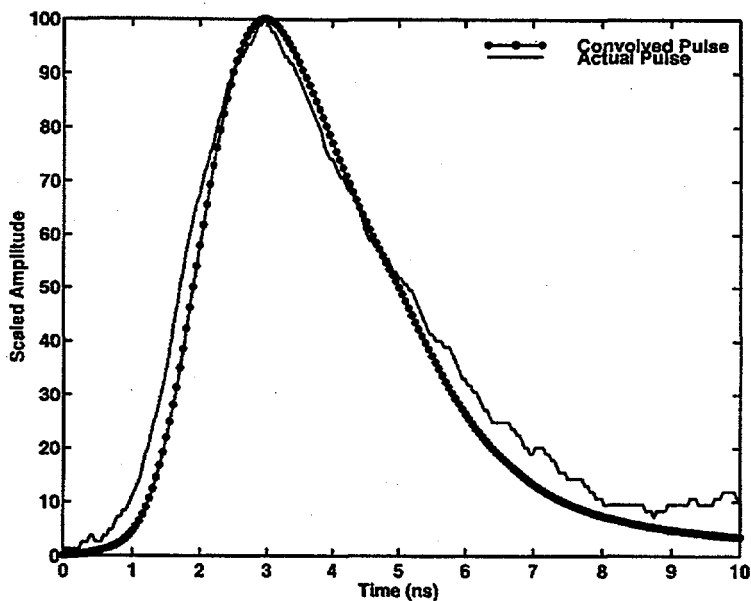


Figure 2.4. Comparison of the Theoretically Expected Response of the PMT/Scintillator System with the Average Pulse Shape Actually Observed in Experiments

An overall evaluation of the initial approach to DFND was performed using pulses whose identity was known a priori via time-of-flight discrimination. Only in this way is it possible to arrive at a set of pulses known to consist entirely of neutron events. (Accidentally coincident events that lead to the misidentification of an interaction are possible, but statistically unlikely.) Figure 2.5 contains histograms of the pulse FWHM for sets of 100 neutron and gamma ray pulses. A relatively weak ^{252}Cf source was

used for these measurements. Three conclusions are possible from this data. First, there is a significant difference between the population of neutron events and the population of gamma-ray events. This difference supports our claim that multiple-proton-recoil pulse discrimination in solid plastic scintillator is at least theoretically possible. A second conclusion is that the majority of neutron pulses are indistinguishable from gamma-ray pulses by any discrimination algorithm. This conclusion is also expected since the vast majority of neutron interactions in a 5-cm diameter, 7.5-cm long cylinder of plastic scintillator consist of only one proton recoil. Clearly, the lack of a second recoil makes recognition of a neutron event impossible. This conclusion indicates that high efficiency neutron detection will require the use of larger amounts of scintillator. Figure 2.6 shows the average pulse shape of the widest 7 % of the 100 neutron pulses compared with the average shape of the widest 7 % of the gamma-ray pulses. This fraction was chosen for display because our MCNP calculations indicate that on average 7 % of the neutron pulses will undergo detectable multiple proton recoil for this geometry. A final conclusion is that even those neutron events that are distinct from gamma-ray events are probably not sufficiently distinct to allow for the nearly total gamma-ray rejection that is required of practical neutron detectors. It is for this reason that a number of "advanced" approaches to multiple-recoil DFND were considered. Our investigation of these advanced approaches is the subject of the next section.

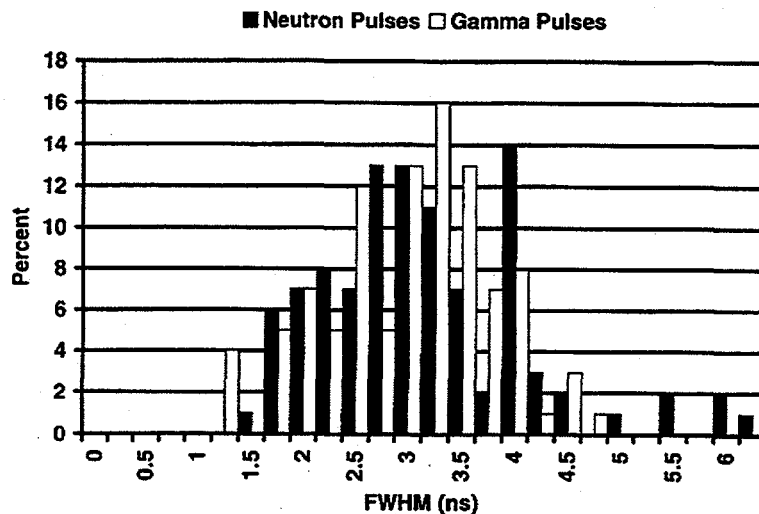


Figure 2.5. Histogram of the Pulse Widths for Sets of 100 Neutron and Gamma-Ray Pulses. The pulses were generated using a ^{252}Cf source and identified a priori using time-of-flight discrimination.

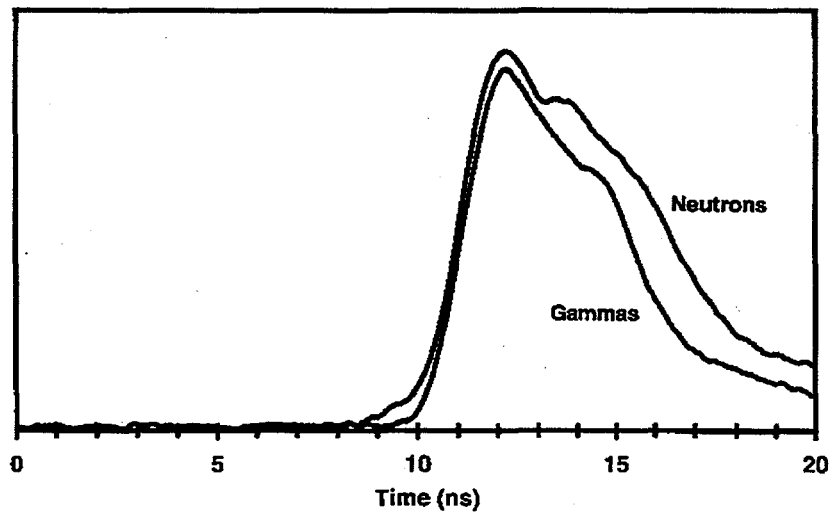


Figure 2.6. Average Pulse Shape for the Widest 7 % of the Pulses Used for Figure 2.5. This fraction corresponds to the fraction of neutron interactions that should consist of multiple recoils.

3.0 Advanced Approaches

The limited success of the initial approach to DFND discussed in the previous section has led to a number of advanced approaches intended to improve gamma-ray-pulse discrimination. These methods can be roughly divided into two categories. The first category retains the use of ordinary, solid plastic scintillator, but acquires pulses whose shapes more accurately reflect the underlying interaction. The second category of methods involves the use of low-density assemblies of plastic scintillator. This strategy lengthens the interaction time for both neutrons and gamma rays, allowing conventional electronics to more easily recognize neutron events.

The improved performance of any advanced approach is, of course, not gained without some sacrifice in the form of reduced efficiency or increased cost. However, it is our assessment that the benefits of DFND are such that field applications would easily be found even for the advanced approaches. The majority of the approaches discussed in this section are planned for investigation early in FY99.

3.1 Multiple PMT Correlation

It was hoped that the degree of correlation between the signals from the two PMTs viewing a single piece of scintillator would provide an indicator as to the identity of the interacting particle. An understanding of this connection can be found by considering the source of the pulse-to-pulse shape variations observed in Figure 2.2. These variations are believed to arise from the random nature of the light emission and collection process. As a result, the variations between gamma-ray pulses acquired by two different PMTs viewing the same scintillator should be relatively uncorrelated. In contrast, a significant part of the pulse-to-pulse variation observed for multiple-recoil neutron pulses arises from the random nature of the neutron interaction. As a result, the degree of correlation between two neutron pulses should be significantly higher for neutron pulses than for gamma-ray pulses.

In practice, this method provided interesting data, but does not appear to offer a simple method for improving pulse-shape discrimination. Figure 3.1 compares a set of pulse pairs obtained for known gamma-ray interactions with pulse pairs for known neutron interactions (time-of-flight pre-identification of interacting particles was again used). The neutron pulses were selected to be those for which significantly correlated pulse shapes most strongly suggest a neutron identity. The gamma-ray pulses were randomly selected. As before, it should be noted that only 7% of ^{252}Cf fission neutrons interacting in this scintillator are expected to undergo multiple neutron recoils. For this reason, the majority of neutron pulses are completely indistinguishable from gamma-ray pulses.

3.2 Fast PMT Tubes

Photek Corporation has recently made available a new type of PMT referred to as a microchannel plate photomultiplier tube (MCP-PMT). In a conventional PMT, photoelectrons accelerate and multiply within a substantial region of space containing the dynode string. In an MCP-PMT, this region is functionally replaced with one or more microchannel plates, wafer-thin devices capable of amplifying an electron signal by 10^3 to 10^4 . (Moszynski et al. 1982; Peurrung and Fajans 1993) Because the MCP itself is quite fast, and the spatial acceleration regions can be vastly reduced in size when using planar MCPs, the MCP-PMT is substantially faster than conventional PMTs such as those normally used for DFND studies. This faster signal acquisition may allow for clearer recognition of multiple-recoil neutron events. The primary drawback to MCP-PMTs is their cost. Currently, an MCP-PMT capable of replacing a single 5-cm PMT costs more than \$10K. While this cost would certainly drop should a large number of MCP-PMTs be required, the microchannel plate itself is a mass-produced item whose cost is not likely to drop below \$1000.

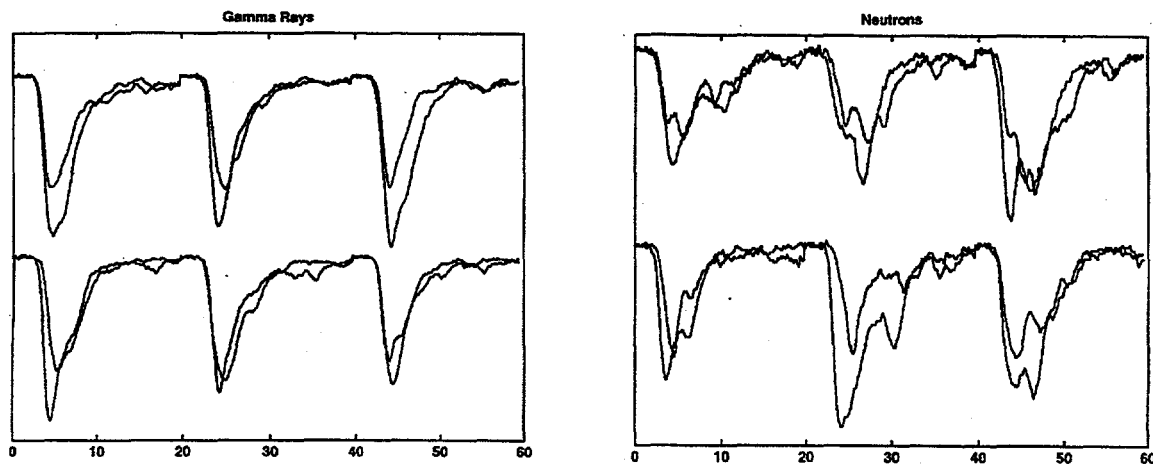


Figure 3.1. Neutron and Gamma-Ray Pulse Pairs for Bicron BC418 Plastic Scintillator. The pulses are obtained from two different PMTs viewing opposite ends of a 5-cm-diameter, 7.5-cm-long piece of scintillator.

3.3 Fast Scintillator

An obvious approach to improving the performance of DFND systems is to use a faster scintillator. Tests with quenched Bicron plastic scintillator were mentioned in the previous section. Unfortunately, the speed of Bicron's quenched scintillator comes with a severe reduction in the light output. Two new attempts to acquire suitable faster scintillators have been undertaken. The first of these involved the scintillator UPS-91F, manufactured by Amcrys-H of the Ukraine. While this scintillator is claimed to have a 0.7 ns rise time similar to Bicron's quenched scintillator, it is also claimed to have a light output nearly four times higher. Our tests found that this scintillator was in reality not quite as fast as Bicron's standard plastic scintillators, but did have quite a high light output. A notable advantage of this Ukrainian scintillator was its low cost. The second effort involves cooperation with Larry Harrah of Adherent Technologies of Albuquerque, New Mexico, who is developing a novel fast scintillator. This scintillator is based upon a fundamentally new set of scintillants and waveshifters capable of much faster light output than the currently available plastic scintillators. We plan to characterize this scintillator when it becomes available in the near future.

3.4 Low-Density Scintillating Assemblies

Both the neutron and gamma-ray interaction timescale depend inversely on the density of scintillators of fixed composition. This is a simple result of the increased distance traveled between interactions in scintillators of lower density. Were it possible to use lower density scintillators, this principle could provide a method to improving the ease with which neutron and gamma-ray pulses can be recognized. Since the density of conventional plastic scintillators is relatively invariant, we are forced to consider the use of assemblies of plastic scintillator with a lower average density. The assembly could take the form of a set of parallel slabs, a hollow cylinder, a hollow sphere, a hollow cube, a periodic array of cylinders, or similar geometry. The remainder of this section describes the design and expected performance of such assemblies. As of 9/1/98, the equipment necessary for a laboratory test of the principles described in this subsection has been ordered. Actual tests are expected early in FY99.

It is important to assess the advantages and disadvantages of the low-density approach to DFND before designing actual systems. The currently known advantages and disadvantages are analyzed and discussed separately below:

Advantages

- **Unlimited Size:** Using low-density scintillators avoids the limitation on the potential size of a single DFND detector. This limitation arises from the optical delay caused by the travel time of scintillation light within the scintillator at a speed of roughly 20 cm/ns. Some of the light created by a particle interaction travels a relatively short distance straight toward the PMT. Other light may travel a circuitous route involving reflection from one or more of the scintillator surfaces. For a scintillator of 10-cm size, such a disparity in light paths may broaden the light pulse by 2 ns or more. Thus, discrimination between neutron and gamma-ray pulses becomes physically impossible for scintillators with sizes above a certain threshold. (Of course, many individual DFND detectors may comprise a system in much the same way that ^3He tubes are used.) Low-density scintillators, in contrast, can be as large as desired since the ability to discriminate neutrons from gamma rays improves with increases in size.
- **Geometric Efficiency:** Since low-density scintillator assemblies may be relatively large, the geometric efficiency presented to a particular source may be substantial. (Geometric efficiency describes the fraction of source neutrons that pass through a detector located at a distance.)
- **Directionality:** Because a low-density scintillating assembly consists of discrete segments with separate PMTs, it is relatively straightforward to acquire information about the incident direction of detected neutrons. A particular scheme that accomplishes this is shown in Figure 1.2.

Disadvantages

- **Detection Efficiency:** The detection efficiency for low-density scintillator assemblies is limited by the fact that multiple-recoil neutron events are not detected if they do not interact within different segments of the assembly. While a scintillating assembly cannot record these neutrons, it should be noted that such events are predominantly those for which the distance between recorded events is relatively small. These same neutrons would be the most likely to be missed even with the initial approach using solid plastic scintillators.
- **Cost:** The cost of DFND systems using scintillating assemblies may be higher than the cost expected using the initial approach. This cost increase results from the need for a larger number of PMTs. However, it should be noted that the geometric efficiency of low-density assemblies is sufficiently high that the overall neutron detection cost per unit of neutron detection "power" may continue to be reasonably low.
- **High-Rate Sensitivity:** Because low-density scintillator assemblies consist of relatively large individual pieces of scintillator, they are more vulnerable to accidental neutron counts resulting from chance coincidence of gamma-ray events. The degree to which this represents a serious problem for DFND will be studied in the coming months after a laboratory test system is constructed.

The design of low-density scintillating assemblies for DFND must be predicated upon an excellent understanding of the physics of proton recoil. Under the reasonable approximation that the mass of the proton and the mass of the neutron are equal, the physics of neutron-proton collisions becomes identical to that of classical spheres with zero moment of inertia ("billiards"). Figure 3.2 shows the assumed geometry for a neutron-proton collision. A neutron incident from the right with energy E_0 strikes a proton that is approximately at rest. The neutron has equal probability of losing any energy

between 0 and E_0 . Forward scattering corresponds to the limit in which the neutron loses little energy. In this case (a “grazing” collision), the proton travels at 90 degrees to the incident-neutron direction with whatever energy is lost by the neutron. In the opposite limit (a “head-on” collision), the neutron loses nearly all of its energy and subsequently travels in a direction nearly perpendicular to its incident direction. The polar plot in Figure 3.2 indicates the probability of neutron scattering as a function of the angle between the outgoing and incoming neutron directions. The mathematical function that describes this probability distribution is $P(\theta) = \sin(2\theta)$, where θ is the scattering angle. From this plot, we see that both the grazing and the head-on collisions are relatively rare. Exactly half of incident neutrons scatter through an angle between 30 and 60 degrees. Only 14% of scattering events involve angles less than 15 degrees or greater than 75 degrees. Note that in no case can a neutron be scattered backwards by a proton recoil. Carbon and other higher-Z elements can, of course, scatter neutrons through angles greater than 90 degrees. However, such collisions are relatively uncommon due to the higher scattering cross section of the proton.

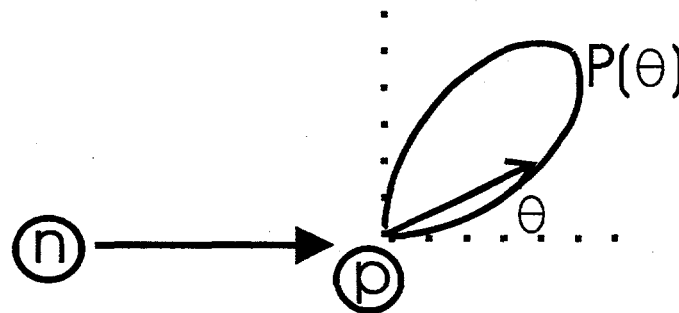


Figure 3.2. Geometry for Neutron-Proton Recoil Events, Along with a Polar Plot of the Scattering Probability as a Function of Scattering Angle

The design of low-density DFND systems must also take into account the accuracy with which gamma-ray interactions can be timed. In practice, it is necessary for fewer than 1 in 10,000 gamma-ray interactions to be mistakenly identified as a neutron interaction. Suppose that the timing of 1 in 10,000 gamma-ray interactions is certain only to within 5 ns. Clearly, a DFND system must ensure that the recoil events of a multiple-recoil neutron interaction are separated by at least 5 ns for this case. A gamma-ray time-of-flight spectrum obtained using a ^{60}Co source is shown in Figure 3.3. Because all gamma rays travel at the same speed, broadening of the time-of-flight spectrum can result only from effects within the scintillator. We have verified that the shape shown in Figure 3.3 does not depend on the local environment of the source or scintillator. Both the accidental coincidence background (distinguished by its time-independence) and the natural neutron background (measured without the source) have been subtracted from the spectrum shown in Figure 3.3. Analysis of this spectrum indicates that 99.99+% of gamma-ray interactions can be timed to within 4 ns. While future studies are planned to improve this performance, it is satisfactory to permit the design of DFND systems using low-density scintillating assemblies. A 1.0 MeV neutron travels only 5.5 cm during 4 ns.

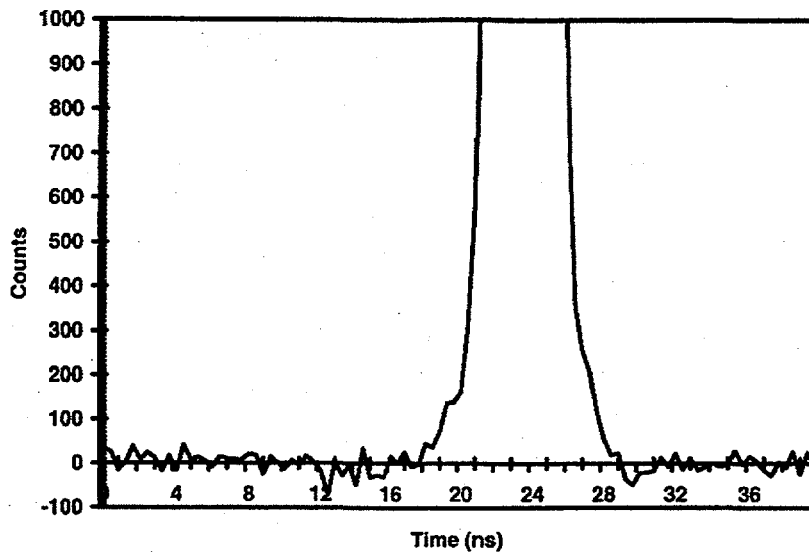


Figure 3.3. Gamma-Ray Time-of-Flight Spectrum Obtained for a ^{60}Co Source with the Hardware and Electronics Anticipated for DFND Systems

Several investigations were carried out to look for unanticipated problems with our low-density assembly approach to DFND. An example of the results of these investigations is shown in Figure 3.4. This figure shows the time-of-flight spectrum between two 10-cm \times 10-cm \times 1.5-cm slab-shaped scintillators when irradiated by a ^{252}Cf fission source. The arrangement of the two scintillators and the source is also indicated in Figure 3.4. The distinct "peaks" in this time-of-flight spectrum are numbered 1 through 5 going from left to right. The tallest, narrowest peak in the center corresponds to events in which a gamma-ray interaction occurs in each scintillator. Such interactions may either result from the same or separate gamma rays. Either way, the high speed of gamma rays leads to nearly simultaneous interactions.

Peaks one and two correspond to events where the interaction occurs first in the left scintillator. Peak number two corresponds to events where a single neutron recoils first in the left and subsequently in the right scintillator. The average energy of the once-scattered neutrons represented in peak 2 is 0.72 MeV. Peak number 1 probably contains a variety of events, but is believed to consist primarily of events in which a gamma-ray interacts first in the left scintillator (because it is faster), followed by a neutron interaction in the right scintillator. Peaks 4 and 5 correspond to peaks 1 and 2 with the order of interaction reversed. The average energy of the once-scattered neutrons represented by peak 4 is 0.93 MeV. Note that the angle through which left-right (peak 2) neutrons must scatter is larger than the angle for right-left (peak 4) neutrons. For the indicated geometry, the vast majority of scattered neutrons will scatter through angles greater than 45 degrees. Remembering the physics of proton recoil, we thus conclude that both the abundance and energy of neutrons in peak 2 should be lower. These predictions are confirmed by the data. The detection system used for this investigation is arguably a functioning DFND detection system. Clearly, such a system can tell the difference between neutron and gamma-ray sources. It can further make inferences about the energy and direction of such sources. While these results are encouraging, this system is very far from an optimized detector. The geometry is particularly inefficient, and we have made no firm effort to demonstrate adequate gamma-ray rejection. We expect these things to be achieved once an optimized system is constructed.

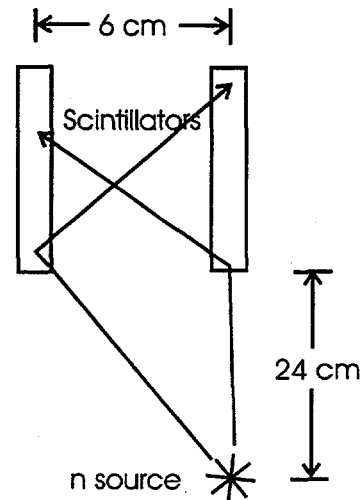
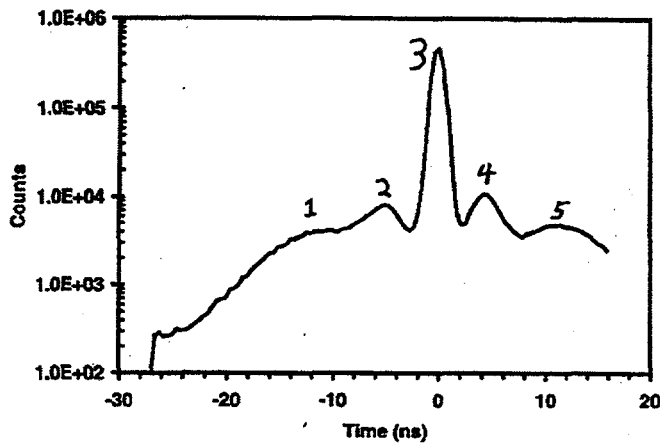


Figure 3.4. Crude Demonstration of DFND Detection Obtained Using Two 10-cm \times 10-cm \times 1.5-cm Scintillating Slabs and a ^{252}Cf Source. The arrangement of the scintillators and the source is shown on the right.

A number of geometries are possible for low-density DFND systems. All that is required of a particular implementation is that multiple recoil events that cross a significant air gap are likely. A list of possible geometries along with a brief description of each is given below:

- **Nearly Conventional:** A large number of thin slabs or disks separated by thin air gaps could be used to assemble a cube or cylinder of scintillator that is an excellent functional approximation of a "low-density" scintillator. PMTs would view such an assembly in much the same way as a solid scintillator.
- **Hollow Cylinder:** A hollow scintillating cylinder could function as a DFND system. The "corners" near the top and bottom surfaces would represent problem areas where multiple-recoil interactions might occur too rapidly to be recognized as such. This geometry is quite amenable to PMT attachment, although the PMTs would necessarily have to be on the outside.
- **Hollow Sphere:** A hollow sphere is perhaps the most technically "ideal" geometry. We have performed substantial modeling to optimize the design of spherical geometries. It would be possible to attach PMTs to the inside of the sphere to reduce the overall device size. The absence of corners on a sphere maximizes the chances that multiple-recoil events will be protracted enough for automated recognition. It should be further noted that the sphere is well suited for the use of waveshifting scintillator. A "band" of waveshifter around the equator of the sphere would gather light that could then be redirected to only one or two PMTs. The sphere is also the only geometry that would allow for 4π -steradian directional sensitivity should that be desired.
- **Slabs:** A number of scintillating slabs can be arranged in a variety of possible geometries. This method has the possible advantage that a large number of identical units are used, simplifying construction. It is also possible to simply use two large slabs, each of which is instrumented with a number of PMTs.

- **Rods:** A regular array of scintillating rods would also make a viable DFND geometry. This method again has the advantage of using a simple basic detection "unit." Rods are particularly well suited for mating to PMTs.

The geometry that we have chosen for an early-FY99 demonstration of the low-density approach to DFND consists of two sizable slabs separated by a sufficient distance to permit time-of-flight recognition of neutron events. There were several reasons for this choice. The two-slab geometry can be easily studied and optimized with ease using MCNP calculations. It should be relatively easy to use the two-slab DFND detector for directional detection of remote fast-neutron sources. Finally, the two-slab geometry can be scaled up with relative ease compared to some of the other geometries.

A calculation of the detection efficiency for the two-slab DFND geometry requires an analysis of the severity of edge effects and an optimization of the thickness of the front and back scintillators. We use the terms "front" and "back" since we here assume that the direction of the source is either known, or that it is desired to find the direction of the source. In either case, it can be assumed that the fast neutron flux to be measured comes from a particular direction. (The direction of an unknown source could rapidly be located by rotating the detector until the signal is maximized. Other, more sophisticated methods are also possible.)

The term, "edge effects," here refers to those neutrons that recoil within the front scintillator, but scatter into a direction that does not cross the back detector. Recall that neutrons primarily scatter through angles between 30 and 60 degrees. The calculated fraction of detected neutrons is shown in Figure 3.5 as a function of the dimensionless ratio of the slab edge length (assuming a square shape) to the separation distance between the slabs. Clearly, few neutrons are lost for slabs that are separated by a distance that is small compared to their sizes. Edge effects, however, become severe for slabs that are relatively well separated. The curve given in Figure 3.5 guides the detector designer who needs to minimize the severity of edge effects subject to the other constraints imposed by the need to ensure successful gamma-ray rejection.

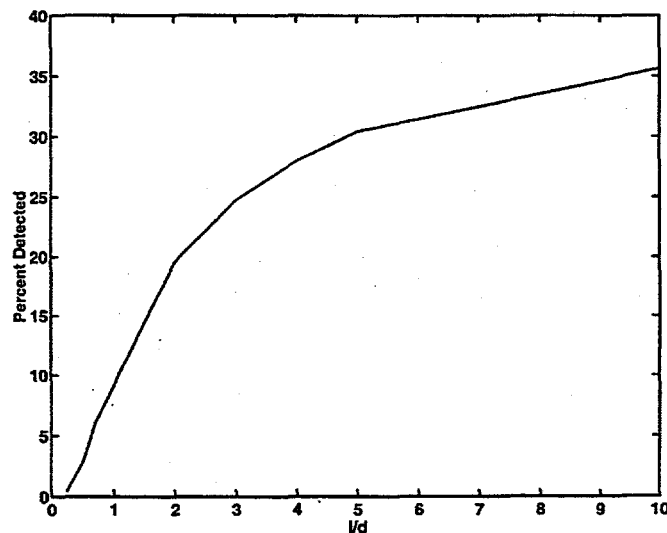


Figure 3.5. Percent of Neutrons that is Detected as a Function of the Dimensionless Ratio of the Square Slab Edge Length, l , to the Separation Distance, d , Between the Slabs. The neutrons are assumed to be normally incident onto the front scintillating slab of optimal thickness. These data are the result of MCNP calculations.

The thickness of the front scintillating slab has an optimum value as shown in Figure 3.6. The calculated detection efficiency shown in this figure assumes that 1.0-MeV neutrons are normally incident and that the scintillator has the composition and density typical of Bircon plastic. It is assumed that detected neutrons deposit at least 100 keV of energy in both the front and back slabs. The existence of an optimum is easy to understand. A front plane that is too thin will allow too many neutrons to simply pass through without interacting. Once a neutron has passed through the front plane, it cannot return since scattering through an angle greater than 90 degrees is impossible unless a carbon nucleus is encountered. (Since the recoil carbon nucleus emits very little light, such events cannot be detected anyway.) On the other hand, a front plane that is too thick will block neutrons from ever reaching the back plane or remove too much of their energy through multiple recoil events before they ever get there. Figure 3.6 indicates that the optimum thickness for the front slab is 3 to 4 cm. A similar calculation assuming 2.0 MeV incident neutrons resulted in an optimum thickness of 4 cm.

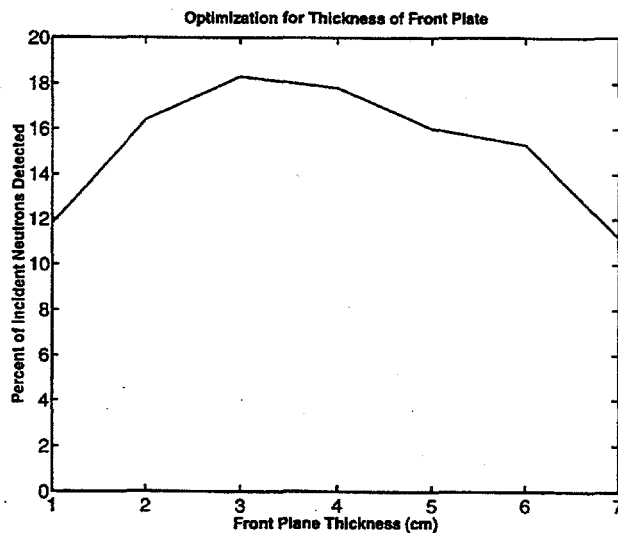


Figure 3.6. Calculated Detection Efficiency of a Two-Slab DFND System as a Function of the Thickness of the Front Slab. The back slab is assumed to be very thick.

There is no optimum thickness for the back scintillating plane; thicker is always better. The function of the back scintillator is to record those neutrons that have already recoiled at least once within the front plane. Figure 3.7 shows the calculated relative efficiency of the two-slab DFND system as a function of the thickness of the back plane. The efficiency is normalized to the efficiency that is obtained when an infinitely thick back plane is used. This graph shows that a back plane that is 5 to 6 cm thick is at least 90% as efficient as the maximum that can be obtained.

The slabs to be tested at PNNL are sized $30 \times 30 \times 4$ cm and $30 \times 30 \times 6$ cm for the front and back scintillators, respectively. It should be possible to operate this DFND system with a total of 8 PMTs, although efficiency may improve should 18 PMTs be used. Understanding how the efficiency depends on the number, locations, and types of PMTs used is one of the main goals of the tests planned for FY99. Further goals are to verify the expected efficiency and the role of edge effects. The ability of this detector to locate a neutron source will also be tested. Finally, a demonstration of satisfactory gamma-ray pulse discrimination will be completed.

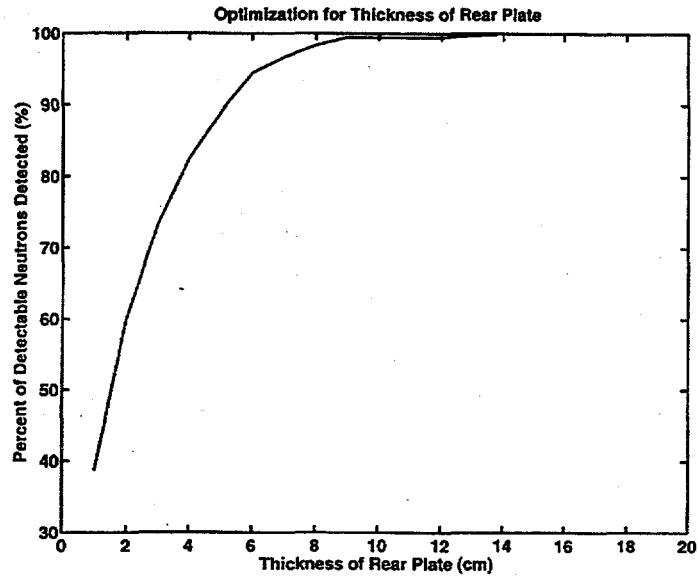


Figure 3.7. Calculated Relative Detection Efficiency of a Two-Slab DFND System as a Function of the Thickness of the Back Scintillator. The optimal thickness is assumed for the front scintillator.

4.0 Conclusion

Two years of work has allowed us to develop a profound insight into the physics of direct fast-neutron detection systems. While a system suitable for use in field applications has not yet emerged, the knowledge and tools necessary to achieve that goal are nearly at hand. The approaches used to allow recognition of neutron pulses and discrimination against gamma-ray pulses are conveniently divided in two. Initial attempts used solid pieces of plastic scintillator and fast, but conventional, electronics. Ultimately, it was found that the differences between the neutron and gamma-ray pulses could not be recognized sufficiently well in the presence of unavoidable, statistical pulse-shape fluctuations. While some neutron pulses are recognizable, gamma-ray pulses mimic neutron pulses at a small, but unacceptable rate. A secondary effort to exploit a variety of advanced approaches is currently underway. Among these approaches is an attempt to exploit the longer interaction times of low-density scintillating assemblies. Both faster scintillators and faster PMTs are also being considered to improve the ease with which pulse-shape discrimination can be performed.

The short-term goals for continuing DFND research are summarized below:

- Determine whether novel fast scintillators from Adherent Technologies Corporation allow the construction of viable DFND systems using solid plastic scintillator.
- Determine whether ultra-fast MCP-PMTs allow construction of viable DFND systems.
- Construct and assess the performance of a two-slab low-density DFND system.
- Demonstrate neutron detection with satisfactory gamma-ray pulse discrimination using at least one of the above strategies.
- Understand the performance of DFND systems in sufficient detail to allow design of systems optimized for particular applications.

5.0 References

- Atwater HF. 1972. "Monte Carlo calculation of recoil spectra in ^4He proportional counters," *Nucl. Instrum. and Meth.*, **100**, 453.
- Bramblett RL, RI Ewing, and TW Bonner. 1960. "A new type of neutron spectrometer," *Nucl. Instrum. And Meth.*, **9**, 1.
- Briesmeister J (Editor). 1993. *MCNP – A General Monte Carlo Code N-Particle Transport Code*, Version 4A, LA-12625-M, Los Alamos National Laboratory, Los Alamos, New Mexico.
- Codino A. 1998. "Gallium arsenide strip detectors for particle identification by the triple measurement of time of flight, position and specific ionization," *Nuclear Physics B* **61** 295.
- Curie I and F Joliot. 1932. "Émission de protons de gran vitesse par les substances hydrogénées sous l'influence des rayons y très pénétrants," *Cont. Rend.* **194** 273.
- Fisher RK, VS Zaveryaev, and SV Trusillo. 1997. "Threshold Bubble Chamber for Measurement of Knock-on DT Neutron Tails from Magnetic and Inertial Confinement Experiments," *Rev. Sci. Instrum.* **68** 1103.
- Hentley JH, L Brandon, A Galonsky, L Heilbronn, BA Remington, S Langer, A Vander Molen, and J Yurkon 1988. "Particle identification via pulse-shape discrimination with a charge-integrating ADC," *Nucl. Instrum. Meth., A* **263** 441.
- Ing H, RA Noulty, and TD McLean. 1997. "Bubble Detectors – A Maturing Technology," *Radiation Measurements*, **27**, 1.
- Knoll GF. 1989. *Radiation Detection and Measurement*, John Wiley & Sons, Inc., New York.
- Kunze V, W-D Schmidt-Ott, U Bosch-Wicke, R Böttger, and H Klein. 1995. "A Modular 4-Pi Counter For Beta-Delayed Neutrons," *Nucl. Instrum. Meth., A* **361** 263.
- Lynch FJ. 1975. "Basic Limitation of Scintillation Counters in Time Measurements," *IEEE Transactions on Nuclear Science*, **NS-22**, 58.
- Menlove HO. 1979. "Description and Operation Manual for the Active Well Coincidence Counter," Los Alamos National Laboratory Report LA-7823-M.
- Menlove HO. 1981. "Description and Performance Characteristics for the Neutron Coincidence Collar for the Verification of Reactor Fuel Assemblies," Los Alamos National Laboratory Report LA-8939-MS.
- Miller WH, RM Brugger, 1985. "Additional experimental tests of the Bonner sphere neutron spectrometer," *Nucl. Instrum. Meth., A* **236** 333.
- Moszynski M and B Bengtson. 1977. "Light pulse shapes from plastic scintillators," *Nucl. Instrum. Meth. A* **142** 417.
- Moszynski M and B Bengtson. 1979. "Status of timing with plastic scintillation detectors," *Nucl. Instrum. Meth. A* **158** 1.

Moszynski M, J Vacher, and R Odru. 1982. "Application of the HR 400 Microchannel Plate Photomultiplier to Study the Light Pulse Shape from Fast and Slow Scintillators by Means of the Single Photon Method," *Nucl. Instrum. Meth. A* **204** 141.

Moszynski M et al. 1992. "Study of N-Gamma Discrimination by Digital Charge Comparison Method for a Large Volume Liquid Scintillator," *Nucl. Instrum. Meth. A* **317** 262.

Peurrung AJ and J Fajans. 1993. "A Pulsed Microchannel-Plate-Based Non-Neutral Plasma Imaging System," *Rev. Sci. Instrum.*, **64**, 52.

Peurrung AJ, CW Hubbard, RR Hansen, PE Keller, RA Craig, PL Reeder, WK Hensley, and DS Sunberg 1997. *Direct Fast-Neutron Detection: A Status Report*, PNNL-11783, Pacific Northwest National Laboratory.

Rinard PM, KL Coop, NJ Nicholas, and HO Menlove. 1994. "Comparison of shuffler and differential die-away technique instruments for the assay of fissile materials in 55-gallon waste drums," *JNMM*, **22**, 28.

Shleien B (Editor) 1992. *The Health Physics and Radiological Handbook*, Scinta, Inc., Silver Spring Md., p. 234.

Vanier PE, L. Forman, and EC Selcow. 1995. "A Thermal Neutron Imager Using Coded Apertures," *Nuclear Materials Management, Proc. 36th Annual Meeting INMM*, Palm Desert, **24** 842.

Distribution

No. of
Copies

OFFSITE

2 DOE Office of Scientific and Technical
Communications

Michael O'Connell, NN-20
Forestal Bldg.
U.S. Department of Energy
1000 Independence Ave. SW
Washington, DC 20585-0420

David Spears, NN-20
Forestal Bldg.
U.S. Department of Energy
1000 Independence Ave. SW
Washington, DC 20585-0420

ONSITE

Pacific Northwest National Laboratory

R. J. Arthur	P8-08
R. A. Craig	K5-25
G. B. Dudder (5)	K6-48
R. R. Hansen (10)	P8-20
W. K. Hensley	P8-08
C. W. Hubbard	P8-48
A.J. Peurrung (15)	P8-08
P. L. Reeder (5)	P8-08
D. E. Robertson	P8-20
D. C. Stromswold (5)	P8-08
D. S. Sunberg	P8-08
R. A. Warner	K6-48
Technical Report Files (5)	